Shot noise and tunnel magnetoresistance in multilevel quantum dots: Effects of cotunneling

I. Weymann[1,*] and J. Barnaś[1,2]
[1]*Department of Physics, Adam Mickiewicz University, 61-614 Poznań, Poland*
[2]*Institute of Molecular Physics, Polish Academy of Sciences, 60-179 Poznań, Poland*
(Received 23 October 2007; revised manuscript received 5 January 2008; published 6 February 2008)

Spin-dependent transport through a multilevel quantum dot weakly coupled to ferromagnetic leads is analyzed theoretically by means of the real-time diagrammatic technique. Both the sequential and cotunneling processes are taken into account, which makes the results on tunnel magnetoresistance (TMR) and shot noise applicable in the whole range of relevant bias and gate voltages. Suppression of the TMR due to inelastic cotunneling and super-Poissonian shot noise has been found in some of the Coulomb blockade regions. Furthermore, in the Coulomb blockade regime, there is an additional contribution to the noise due to bunching of cotunneling processes involving the spin-majority electrons. On the other hand, in the sequential tunneling regime, TMR oscillates with the bias voltage, while the current noise is generally sub-Poissonian.

DOI: 10.1103/PhysRevB.77.075305 PACS number(s): 73.63.Kv, 72.25.Mk, 85.75.−d, 73.23.Hk

I. INTRODUCTION

Transport properties of quantum dots coupled to ferromagnetic leads are currently a subject of extensive experimental and theoretical studies.[1–16] This interest is stimulated by expected applications in spintronics and quantum computing.[1–3] When a quantum dot is coupled to two ferromagnetic leads, its transport properties depend on the magnetic configuration of the system. This is the so-called tunnel magnetoresistance (TMR) effect, which is characterized by the ratio $\mathrm{TMR}=(I_P-I_{AP})/I_{AP}$, where I_P (I_{AP}) is the current flowing through the system in the parallel (antiparallel) configuration.[6,8,17] When coupling between the dot and leads is strong, the Kondo physics emerges for $T\lesssim T_K$, where T_K is the Kondo temperature.[4] In turn, single-electron charging in the weak coupling regime leads to the Coulomb blockade phenomenon.[5,6] Sequential (first order) transport is exponentially suppressed in the blockade regime. The current flows then due to cotunneling (second order) processes involving correlated tunneling through virtual states of the dot, whereas outside the blockade regime, transport is dominated by sequential tunneling processes.[18] So far fully systematic considerations (taking into account both sequential and cotunneling processes) of spin-dependent transport through a quantum dot in the weak coupling regime (perturbative regime with respect to the dot-lead coupling) have been restricted mainly to single-level quantum dots.[8] In real systems, however, usually more than one energy level participates in transport, leading to more complex and interesting transport characteristics.[19,20] It has been shown recently that the Fano factor in the Coulomb blockade regime calculated in the first-order approximation is larger than unity.[20] Moreover, the TMR was found then to be independent of the gate voltage. The results for the Coulomb blockade regime obtained by taking into account only the sequential processes are, however, rather not reliable.

In this paper, we therefore extend the existing theoretical studies by including the cotunneling processes. We show that the shot noise in the Coulomb blockade regime can be super-Poissonian, although the Fano factor is significantly reduced by the cotunneling processes. Apart from this, we show that the TMR in the blockade regime is considerably modified by cotunneling processes, and can be either enhanced or reduced in comparison to that in the first-order approximation, depending on the transport regime. Our considerations are based on the real-time diagrammatic technique[8,21,22] which, after taking into account both the first- and second-order contributions, allows us to analyze transport in the *full* weak coupling regime, i.e., in the cotunneling, cotunneling-assisted sequential, and sequential tunneling regimes. Furthermore, to calculate the shot noise in the cotunneling regime, we include the non-Markovian effects,[22] which were neglected in previous considerations.[23]

The paper is organized as follows. In Sec. II, we present details of the model and theoretical method. Section III includes numerical results for the different sets of parameters, corresponding to different dot occupation scenarios. Final conclusions are given in Sec. IV.

II. MODEL AND METHOD

We consider a two-level quantum dot weakly coupled to external ferromagnetic leads whose magnetic moments are either parallel or antiparallel. The Hamiltonian of the system reads $\hat{H}=\hat{H}_L+\hat{H}_R+\hat{H}_D+\hat{H}_T$. The first two terms describe noninteracting itinerant electrons in the leads, $\hat{H}_r=\sum_{\mathbf{k}\sigma}\varepsilon_{r\mathbf{k}\sigma}c^\dagger_{r\mathbf{k}\sigma}c_{r\mathbf{k}\sigma}$ for the left ($r=L$) and right ($r=R$) leads, where $c^\dagger_{r\mathbf{k}\sigma}$ ($c_{r\mathbf{k}\sigma}$) creates (annihilates) an electron with the wave vector $\mathbf{k}$ and spin σ in the lead r, and $\varepsilon_{r\mathbf{k}\sigma}$ is the corresponding dispersion relation. The quantum dot is described by

$$\hat{H}_D=\sum_{j\sigma}\varepsilon_j n_{j\sigma}+U\sum_j n_{j\uparrow}n_{j\downarrow}+U'\sum_{\sigma\sigma'}n_{1\sigma}n_{2\sigma'}, \qquad (1)$$

where $n_{j\sigma}=d^\dagger_{j\sigma}d_{j\sigma}$ and $d^\dagger_{j\sigma}$ ($d_{j\sigma}$) is the creation (annihilation) operator of an electron with spin σ in the jth level ($j=1$ and 2), ε_j is the corresponding single-particle energy, and $U(U')$ is the on-level (interlevel) Coulomb repulsion parameter. The tunnel Hamiltonian, $\hat{H}_T$, takes the form $\hat{H}_T=\sum_{r=L,R}\sum_{\mathbf{k}j\sigma}(t_{rj}c^\dagger_{r\mathbf{k}\sigma}d_{j\sigma}+t^\star_{rj}d^\dagger_{j\sigma}c_{r\mathbf{k}\sigma})$, where t_{rj} is the relevant

tunneling matrix element. Coupling of the jth level to the spin-majority (spin-minority) electron band of the lead r is described by $\Gamma_{rj}^{+(-)}=2\pi|t_{rj}|^2\rho_r^{+(-)}=\Gamma_{rj}(1\pm p_r)$, where $\Gamma_{rj}=(\Gamma_{rj}^{+}+\Gamma_{rj}^{-})/2$, while $\rho_r^{+(-)}$ and p_r are the spin-dependent density of states and spin polarization in the lead r, respectively. In the following, we assume $\Gamma_{rj}\equiv\Gamma/2$ and $p_L=p_R\equiv p$.

In order to calculate the spin-polarized transport through a two-level quantum dot in the sequential and cotunneling regimes, we employ the real-time diagrammatic technique.[8,21,22] It consists in a systematic expansion of the quantum dot (reduced) density matrix and the current operator with respect to the dot-lead coupling strength Γ. The current operator $\hat{I}$ is defined as $\hat{I}=(\hat{I}_R-\hat{I}_L)/2$, with $\hat{I}_r=-i(e/\hbar)\Sigma_{\mathbf{k}\sigma}\Sigma_j(t_{rj}c_{r\mathbf{k}\sigma}^{\dagger}d_{j\sigma}-t_{rj}^{\star}d_{j\sigma}^{\dagger}c_{r\mathbf{k}\sigma})$ being the current flowing from the dot to the lead r. Time evolution of the reduced density matrix can be visualized as a sequence of irreducible self-energy blocks, $W_{\chi\chi'}$, on the Keldysh contour. The matrix elements $W_{\chi\chi'}$ describe transitions between the many-body states $|\chi\rangle$ and $|\chi'\rangle$ of the two-level dot.[20] The full propagation of the dot density matrix is given by the Dyson equation, which is further transformed into a general kinetic equation for the elements of the reduced density matrix. With the aid of the matrix notation introduced in Ref. 22, all the quantities of interest can be defined in terms of the following self-energy matrices: $\mathbf{W}$, $\mathbf{W}^{\mathrm{I}}$, $\mathbf{W}^{\mathrm{II}}$, $\partial\mathbf{W}$, and $\partial\mathbf{W}^{\mathrm{I}}$. The matrix $\mathbf{W}^{\mathrm{I(II)}}$ is the self-energy matrix with one *internal* vertex (two internal vertices) resulting from the expansion of the tunneling Hamiltonian replaced by the current operator, while $\partial\mathbf{W}$ and $\partial\mathbf{W}^{\mathrm{I}}$ are partial derivatives of $\mathbf{W}$ and $\mathbf{W}^{\mathrm{I}}$ with respect to the convergence factor of the Laplace transform.[22] Using the above matrices, the stationary occupation probabilities can be found from $(\tilde{\mathbf{W}}\mathbf{p}^{\mathrm{st}})_{\chi}=\Gamma\delta_{\chi\chi_0}$, where $\mathbf{p}^{\mathrm{st}}$ is the vector containing probabilities and the matrix $\tilde{\mathbf{W}}$ is given by $\mathbf{W}$ with one arbitrary row χ_0 replaced by $(\Gamma,\ldots,\Gamma)$ due to the normalization, $\Sigma_{\chi}p_{\chi}^{\mathrm{st}}=1$. The current flowing through the system can then be found from

$$I=\frac{e}{2\hbar}\mathrm{Tr}\{\mathbf{W}^{\mathrm{I}}\mathbf{p}^{\mathrm{st}}\}. \tag{2}$$

Finally, the zero-frequency current noise, $S=2\int_{-\infty}^{0}dt(\langle\hat{I}(t)\hat{I}(0)+\hat{I}(0)\hat{I}(t)\rangle-2\langle\hat{I}\rangle^2)$, is given by[22]

$$S=\frac{e^2}{\hbar}\mathrm{Tr}\{[\mathbf{W}^{\mathrm{II}}+\mathbf{W}^{\mathrm{I}}(\mathbf{P}\mathbf{W}^{\mathrm{I}}+\mathbf{p}^{\mathrm{st}}\otimes\mathbf{e}^{T}\partial\mathbf{W}^{\mathrm{I}})]\mathbf{p}^{\mathrm{st}}\}, \tag{3}$$

where the object $\mathbf{P}$ is calculated from $\tilde{\mathbf{W}}\mathbf{P}=\tilde{\mathbf{1}}(\mathbf{p}^{\mathrm{st}}\otimes\mathbf{e}^{T}-\mathbf{1}-\partial\mathbf{W}\mathbf{p}^{\mathrm{st}}\otimes\mathbf{e}^{T})$, with $\tilde{\mathbf{1}}$ being the unit vector with row χ_0 set to zero, and $\mathbf{e}^{T}=(1,\ldots,1)$.[22]

To calculate the transport properties order by order in tunneling processes, we expand the self-energy matrices, $\mathbf{W}^{(\mathrm{I,II})}=\mathbf{W}^{(\mathrm{I,II})(1)}+\mathbf{W}^{(\mathrm{I,II})(2)}+\cdots$, the dot occupations, $\mathbf{p}^{\mathrm{st}}=\mathbf{p}^{\mathrm{st}(0)}+\mathbf{p}^{\mathrm{st}(1)}+\cdots$, and $\mathbf{P}=\mathbf{P}^{(-1)}+\mathbf{P}^{(0)}+\cdots$, respectively. The self-energies can be calculated using the corresponding diagrammatic rules.[8,22] The first order of expansion corresponds to the sequential tunneling, whereas the second one to cotunneling. Thus, by taking into account all the first- and second-order contributions, we are able to resolve transport properties in the full range of the bias and gate voltages.

The sequential tunneling dominates transport above a threshold voltage and is exponentially suppressed in the Coulomb blockade regime. In the blockade regime, on the other hand, the dominant contribution to the current comes from cotunneling processes,[18] which take place through virtual states of the system and are only algebraically suppressed in the Coulomb blockade. As we show in the following, to reliably analyze transport properties in the blockade regions, it is necessary to include second-order contributions. We, however, also note that in the limit of $\Gamma\ll k_BT$, the sequential tunneling results may be recovered.[22]

III. NUMERICAL RESULTS

In the following, we present and discuss numerical results on the differential conductance, TMR, and the Fano factor of a two-level quantum dot in the sequential and cotunneling regimes. Depending on the ratio, $U/(\delta\varepsilon+U')$, where $\delta\varepsilon=\varepsilon_2-\varepsilon_1$ is the level spacing, the shell filling sequence of the quantum dot can generally have two different scenarios.

A. Case of $U>\delta\varepsilon+U'$

When $U>\delta\varepsilon+U'$, the lower orbital level of the dot becomes doubly occupied only after the higher orbital level is occupied by a single electron. In other words, in the Coulomb blockade regime with two electrons in the ground state, each electron occupies different orbital levels of the dot. Experimentally, such situation can be realized, for example, in single-wall metallic carbon nanotube quantum dots.[24] Then, the two levels of quantum dot would correspond to the two orbital levels coming from different subbands of the nanotube.

1. Results on tunnel magnetoresistance

The TMR as a function of the bias voltage and position of the dot levels is shown in Fig. 1(b). To facilitate the identification of different transport regimes, we present in Fig. 1(a) the density plot of the differential conductance G in the parallel configuration (differential conductance in the antiparallel configuration is qualitatively similar[20]). Since the position of the dot levels can be shifted with a gate voltage, Figs. 1(a) and 1(b) can be viewed as a bias and gate voltage dependence of G and TMR, respectively. By sweeping the gate voltage in the linear response regime, the number of electrons in the dot can be changed successively. More precisely, this happens when $\varepsilon\equiv\varepsilon_1=0$, $\varepsilon=-(\delta\varepsilon+U')$, $\varepsilon=-(U+U')$, and $\varepsilon=-(\delta\varepsilon+U+2U')$. Thus, for $\varepsilon\gtrsim 0$ $[-(\delta\varepsilon+U+2U')\gtrsim\varepsilon]$, the dot is empty (fully occupied). When $0\gtrsim\varepsilon\gtrsim-(\delta\varepsilon+U')$ $[-(U+U')\gtrsim\varepsilon\gtrsim-(\delta\varepsilon+U+2U')]$, there is a single electron (three electrons) in the dot. On the other hand, for $-(\delta\varepsilon+U')\gtrsim\varepsilon\gtrsim-(U+U')$, the dot is occupied by two electrons, one on each orbital level.

In the case of empty (fully occupied) dot in the Coulomb blockade regime, the current flows only due to elastic non-spin-flip cotunneling processes. Such processes are fully coherent and do not affect the charge and spin state of the dot.

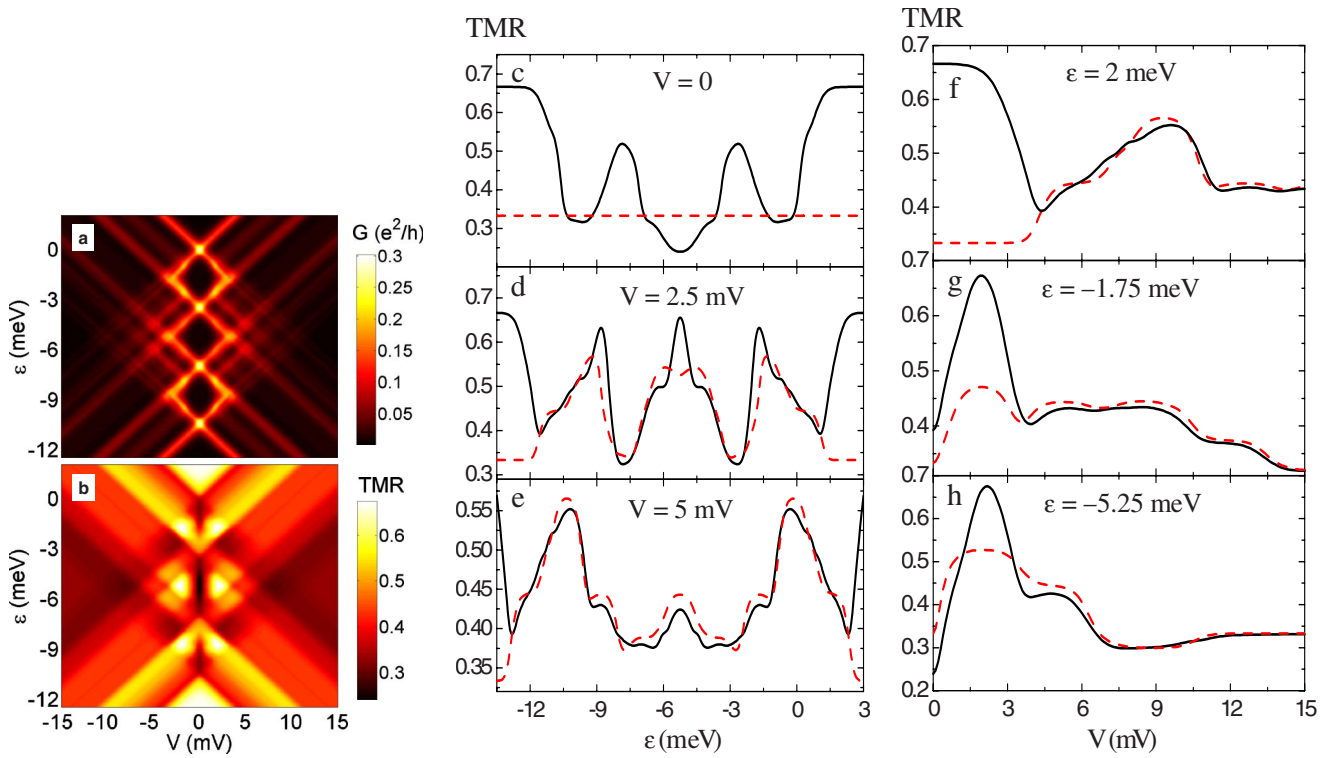

FIG. 1. (Color online) (a) The differential conductance G in the parallel configuration and (b) the TMR as a function of the bias voltage V and level position $\varepsilon=\varepsilon_1$. (c)–(e) show the TMR as a function of ε for several values of V, whereas (f)–(h) display the bias voltage dependence of TMR for several values of ε. The dashed lines in (c)–(h) show the first-order contributions. The parameters are $k_BT=0.15$ meV, $\varepsilon_2-\varepsilon_1=1.5$ meV, $U=5$ meV, $U'=2$ meV, $\Gamma=0.1$ meV, and $p=0.5$.

As a result, the system behaves like a single ferromagnetic tunnel junction, yielding the TMR given by the Julliere formula,[8,17] $\mathrm{TMR}=2p^2/(1-p^2)$. However, in the other blockade regions, both the non-spin-flip and spin-flip cotunneling processes are allowed, leading to the suppression of the TMR. This can be seen in Fig. 1(c), where we plot the gate voltage dependence of the TMR in the linear response regime. When there is a single electron on one of the two orbital levels, the TMR is decreased. This is due to the spin-flip cotunneling processes which provide a channel for spin relaxation, decreasing the difference between conductance in the parallel and antiparallel configurations and, thus, reducing the TMR.[8] On the other hand, in the regime when each dot level is singly occupied (doubly occupied dot), the amount of spin-flip cotunneling is increased and the suppression of TMR is even more pronounced. However, when the bias voltage is increased, the central minimum in TMR [Fig. 1(c)] transforms into a local maximum due to a nonequilibrium spin accumulation in the dot [see Figs. 1(d) and 1(e)].

The bias voltage dependence of the TMR for several values of the level position is displayed in Figs. 1(f)–1(h). When the dot is empty in equilibrium ($\varepsilon=2$ meV), the TMR in the cotunneling regime is given by the Julliere value. However, once the bias voltage reaches the threshold voltage ($V\approx 3$ mV), the sequential processes are allowed and TMR drops [see Fig. 1(f)]. If the ground state is singly occupied ($\varepsilon=-1.75$ meV), a nonequilibrium spin accumulation in doublet states ($p^{\mathrm{st}}_{|\uparrow 0\rangle}\neq p^{\mathrm{st}}_{|\downarrow 0\rangle}$) is built up with increasing bias voltage.[9] This leads to an enhanced TMR, which again starts to drop around the threshold for sequential tunneling [see Fig. 1(g)]. Finally, in Fig. 1(h), we show the bias dependence of TMR for the case when the dot is doubly occupied in equilibrium ($\varepsilon=-5.25$ meV). Now, the spin accumulation in triplet states ($p^{\mathrm{st}}_{|\uparrow\uparrow\rangle}\neq p^{\mathrm{st}}_{|\downarrow\downarrow\rangle}$) gives rise to an increase in TMR.[25] We also note that in the transport regime where the sequential tunneling is allowed, more and more charge states become active in transport with increasing the bias voltage. This gives rise to steplike I-V characteristics and the oscillatorylike behavior of the TMR [see Figs. 1(f)–1(h)].

In Figs. 1(c)–1(h), we also showed the TMR calculated in the first-order (sequential) approximation (dashed lines). It is evident that the role of cotunneling processes is particularly pronounced in the blockade regions, where the cotunneling processes dominate over the sequential ones, and lead to a significant enhancement (or reduction) of TMR. Outside the blockade regions, TMR is determined mainly by sequential transport, so the contribution from cotunneling processes is rather minor.

2. Results on shot noise

Upon calculating the current I and the zero-frequency current noise S, one can determine the Fano factor F, $F=S/2e|I|$. The Fano factor describes the deviation of S from the Poissonian shot noise given by $S_p=2e|I|$. The bias and gate voltage dependence of the Fano factor in the parallel and antiparallel magnetic configurations is shown in Figs.

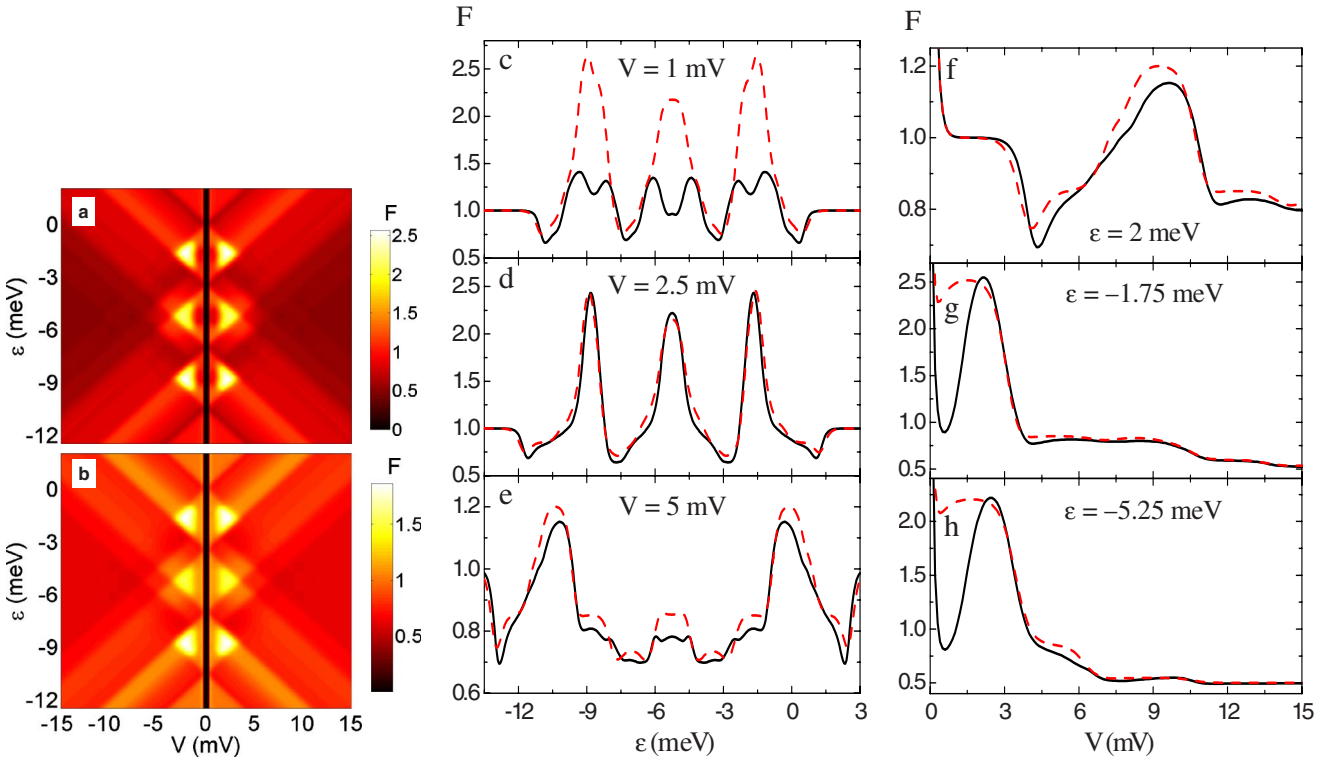

FIG. 2. (Color online) The Fano factor F as a function of the bias voltage and level position for the (a) parallel and (b) antiparallel magnetic configurations. (c)–(h) show F in the parallel configuration as a function of [(c)–(e)] the level position and [(f)–(h)] the bias voltage. The dashed lines present the first-order contributions. The parameters are the same as in Fig. 1.

2(a) and 2(b), respectively. When $|eV| \lesssim k_B T$, S is dominated by thermal Nyquist-Johnson noise; otherwise, the noise due to the discrete nature of charge (shot noise) dominates.[26] In the limit of $V \to 0$, the current tends to zero, whereas the current noise is dominated by thermal noise. This leads to a divergency of the Fano factor in the linear response regime. Therefore, in the density plots of F, we mark the low bias voltage regime with a black line.

In the cotunneling regime, where the dot is empty (or fully occupied), the shot noise is Poissonian [Fig. 2(c)]. This is because the current flows then only due to elastic non-spin-flip second-order processes.[22,23] However, in the Coulomb blockade regions, where inelastic cotunneling processes also contribute, we find a pronounced super-Poissonian shot noise [see Figs. 2(d) and 2(e)]. This increased shot noise is related to bunching of electrons carried by different types of cotunneling processes. Furthermore, in the case of magnetic leads, there is an additional contribution to the noise coming from the difference between the spin-up and spin-down channels, which leads to bunching of fast cotunneling processes involving the majority electrons. This is more pronounced in the parallel configuration, where the difference between the two channels is approximately equal to $(1+p)^2/(1-p)^2$, while for the antiparallel configuration, the two channels are comparable [see Figs. 2(a) and 2(b)]. The variation of the Fano factor with the bias voltage is displayed in Figs. 2(f)–2(h). When the dot is empty [Fig. 2(f)], the Fano factor is Poissonian and starts to drop at the onset of sequential tunneling. With increasing bias voltage, the noise becomes super-Poissonian in some range of the transport voltage. In the case of singly and doubly occupied quantum dots, the bias voltage dependencies of F are qualitatively similar. In the Coulomb blockade regime, the current noise becomes super-Poissonian (up to $F \approx 2.5$ in the parallel configuration), indicating the existence and role of inelastic and spin-flip cotunneling processes.[23] For example, in the case of doubly occupied dot [Fig. 2(h)], the maximum Fano factor is found for voltages where inelastic cotunneling between the two orbital levels is allowed, $|eV| \approx 2\delta\varepsilon$. On the other hand, in the sequential tunneling regime, the Fano factor becomes suppressed and is generally sub-Poissonian due to the Coulomb correlations in sequential transport.[5,20] For comparison, in Figs. 2(c)–2(h), we show the results calculated within the sequential tunneling approximation (dashed lines), which clearly show the role of cotunneling processes in shot noise, particularly in the blockade regions. We also note that the occurrence of super-Poissonian shot noise in the Coulomb blockade regime has also been reported experimentally in quantum dots coupled to nonmagnetic leads.[27–29]

B. Case of $U < \delta\varepsilon + U'$

When $U < \delta\varepsilon + U'$, by sweeping the gate voltage, the consecutive dot orbital level becomes occupied only after the lower lying level is fully occupied, which is characteristic of semiconducting quantum dots.[15,16] In such a case, transport properties of the two-level quantum dot generally resemble

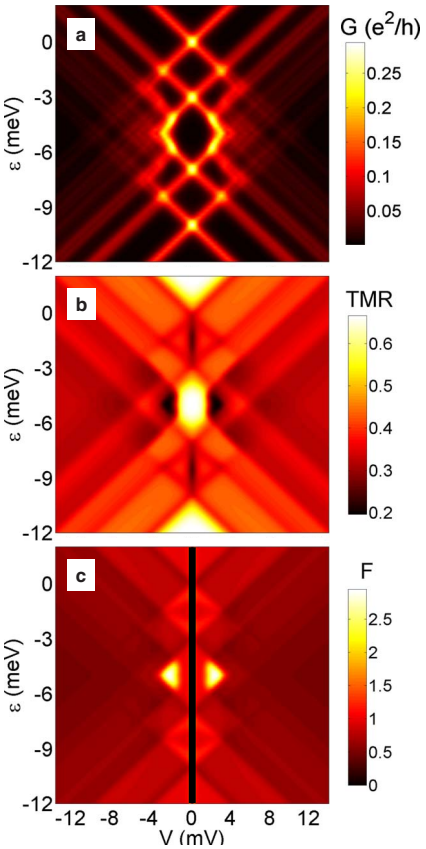

FIG. 3. (Color online) (a) The differential conductance G and (c) the Fano factor in the parallel configuration, and (b) the TMR as a function of the bias voltage V and level position $\varepsilon=\varepsilon_1$. The parameters are $k_BT=0.15$ meV, $\varepsilon_2-\varepsilon_1=U=3$ meV, $U'=2$ meV, $\Gamma=0.1$ meV, and $p=0.5$.

those of single-level quantum dots. However, there are still some differences, as shown below.

In Fig. 3(a), we display the differential conductance in the parallel configuration as a function of the bias and gate voltages. The Coulomb diamonds, particularly the central one, are modified in comparison to those in Fig. 1(a). When changing the gate voltage, the corresponding states of the dot become consecutively occupied, and the dot is empty (fully occupied) for $\varepsilon \gtrsim 0[-(\delta\varepsilon+U+2U') \gtrsim \varepsilon]$; there is a single electron (three electrons) when $0 \gtrsim \varepsilon \gtrsim -U[-(\delta\varepsilon+2U') \gtrsim \varepsilon \gtrsim -(\delta\varepsilon+U+2U')]$. Finally, for $-U \gtrsim \varepsilon \gtrsim -(\delta\varepsilon+2U')$, the first orbital level of the dot is fully occupied, while the second one is empty. The bias and gate voltage dependence of the TMR is shown in Fig. 3(b). In the low bias regime, the behavior of TMR is similar to that of single-level quantum dots.[8] For empty or fully occupied orbital levels, the TMR is given by the Julliere value due to the absence of inelastic spin-flip processes. On the other hand, when the dot occupation number is odd, the TMR is suppressed due to the spin-flip cotunneling. This is the parity effect of the linear response TMR reported in Ref. 8 for single-level quantum dots. In the nonlinear response regime, however, the behavior of TMR becomes more complex as compared to that for single-level dots. This is most pronounced in the case of doubly occupied ground state, $\varepsilon=-5$ meV, as shown in Fig.

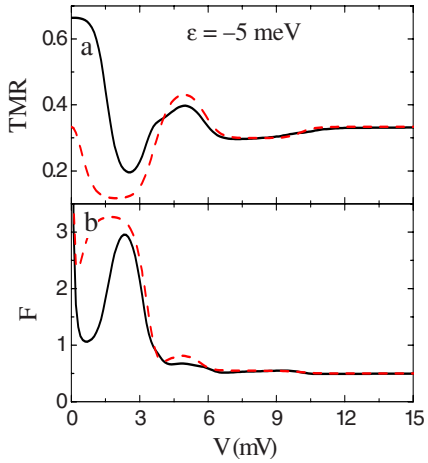

FIG. 4. (Color online) (a) The bias voltage dependence of the TMR and (b) the Fano factor in the parallel configuration for the same parameters as in Fig. 3. The dashed curves show the first-order calculation.

4(a), where the lower orbital level is doubly occupied while the higher one is empty. Now, with increasing bias voltage, close to the resonance, the TMR drops from the Julliere value and becomes considerably suppressed due to the existence of spin-flip cotunneling between different orbital levels.

The density plot of the Fano factor in the case of $U < \delta\varepsilon+U'$ is shown in Fig. 3(c) for the parallel configuration. The dependence of the Fano factor in the antiparallel configuration is qualitatively similar to that in the parallel configuration and, thus, is not shown here. One can see that in the blockade regimes, where the current flows mainly due to elastic cotunneling (regimes with even occupations), and for low bias voltages (but still $|eV| > k_BT$), the shot noise is Poissonian. When the dot occupation is odd, the Fano factor in the Coulomb blockade becomes slightly larger than unity, but this effect is, however, rather unnoticeable. On the other hand, in the nonlinear response regime for doubly occupied dot, we find a large super-Poissonian shot noise. This is shown in Fig. 4(b), where the bias dependence of the Fano factor is displayed for $\varepsilon=-5$ meV. The super-Poissonian shot noise is due to the interplay between the elastic and inelastic cotunnelings and due to bunching of inelastic processes through different orbital levels. In addition, in Fig. 4, we also show the results calculated within the sequential tunneling approximation. Again, the effect of cotunneling is most visible and important in the Coulomb blockade regimes, whereas in the sequential tunneling regime, the cotunneling processes only slightly modify transport properties of the system.

IV. CONCLUDING REMARKS

In conclusion, we have considered spin-polarized transport through a two-level quantum dot coupled to ferromagnetic leads in the sequential and cotunneling regimes. We have analyzed the dependence of the TMR and Fano factor on the bias and gate voltages. Furthermore, we have consid-

ered two different sets of parameters, corresponding to different dot occupation scenarios (the first one may correspond to quantum dots based on single-wall metallic carbon nanotubes, whereas the second one to semiconducting quantum dots). In the first case, we have found a suppression of TMR in the Coulomb blockade regime for singly and doubly occupied quantum dots. Furthermore, the inelastic cotunneling processes in these transport regimes lead to super-Poissonian shot noise, irrespective of magnetic configuration of the system. On the other hand, in the second case, the transport properties of the system generally resemble those of single-level quantum dots except for the nonlinear response regime with doubly occupied ground state. In this transport regime, we find a suppression of the TMR and super-Poissonian shot noise due to inelastic spin-flip cotunneling. We also note that the current noise is generally sub-Poissonian in the sequential tunneling regime, while TMR exhibits oscillatorylike dependence on the bias voltage, irrespective of the choice of parameters. Finally, we notice that the sequential tunneling approximation in the Coulomb blockade regime generally underestimates the TMR and overestimates the Fano factor.

ACKNOWLEDGMENTS

We acknowledge discussions with A. Thielmann. This project was supported by funds of the Polish Ministry of Science and Higher Education as a research project in years 2006–2009. I.W. acknowledges support from the Foundation for Polish Science.

*weymann@amu.edu.pl

[1] S. Maekawa and T. Shinjo, *Spin Dependent Transport in Magnetic Nanostructures* (Taylor & Francis, London, 2002).
[2] I. Zutic, J. Fabian, and S. Das Sarma, Rev. Mod. Phys. **76**, 323 (2004).
[3] K. Yakushiji, F. Ernult, S. Mitani, K. Takanashi, and H. Fujimori, Phys. Rep. **451**, 1 (2007).
[4] J. Martinek, Y. Utsumi, H. Imamura, J. Barnaś, S. Maekawa, J. König, and G. Schön, Phys. Rev. Lett. **91**, 127203 (2003); M.-S. Choi, D. Sanchez, and R. Lopez, *ibid.* **92**, 056601 (2004).
[5] M. Braun, J. König, and J. Martinek, Phys. Rev. B **70**, 195345 (2004); **74**, 075328 (2006).
[6] W. Rudziński and J. Barnaś, Phys. Rev. B **64**, 085318 (2001).
[7] A. Cottet, W. Belzig, and C. Bruder, Phys. Rev. B **70**, 115315 (2004); Phys. Rev. Lett. **92**, 206801 (2004).
[8] I. Weymann, J. König, J. Martinek, J. Barnaś, and G. Schön, Phys. Rev. B **72**, 115334 (2005).
[9] I. Weymann, J. Barnaś, J. König, J. Martinek, and G. Schön, Phys. Rev. B **72**, 113301 (2005).
[10] A. Cottet and M.-S. Choi, Phys. Rev. B **74**, 235316 (2006).
[11] M. M. Deshmukh and D. C. Ralph, Phys. Rev. Lett. **89**, 266803 (2002).
[12] S. Sahoo, T. Kontos, J. Furer, C. Hoffmann, M. Gräber, A. Cottet, and C. Schönenberger, Nat. Phys. **1**, 102 (2005).
[13] H. B. Heersche, Z. de Groot, J. A. Folk, L. P. Kouwenhoven, H. S. J. van der Zant, A. A. Houck, J. Labaziewicz, and I. L. Chuang, Phys. Rev. Lett. **96**, 017205 (2006).
[14] A. Bernand-Mantel, P. Seneor, N. Lidgi, M. Munoz, V. Cros, S. Fusil, K. Bouzehouane, C. Deranlot, A. Vaures, F. Petroff, and A. Fert, Appl. Phys. Lett. **89**, 062502 (2006).
[15] K. Hamaya, S. Masubuchi, M. Kawamura, T. Machida, M. Jung, K. Shibata, K. Hirakawa, T. Taniyama, S. Ishida, and Y. Arakawa, Appl. Phys. Lett. **90**, 053108 (2007).
[16] K. Hamaya, M. Kitabatake, K. Shibata, M. Jung, M. Kawamura, K. Hirakawa, T. Machida, T. Taniyama, S. Ishida, and Y. Arakawa, Appl. Phys. Lett. **91**, 022107 (2007); **91**, 232105 (2007).
[17] M. Julliere, Phys. Lett. **54A**, 225 (1975).
[18] D. V. Averin and Yu. V. Nazarov, Phys. Rev. Lett. **65**, 2446 (1990); K. Kang and B. I. Min, Phys. Rev. B **55**, 15412 (1997).
[19] W. Belzig, Phys. Rev. B **71**, 161301(R) (2005).
[20] I. Weymann and J. Barnaś, J. Phys.: Condens. Matter **19**, 096208 (2007).
[21] H. Schoeller and G. Schön, Phys. Rev. B **50**, 18436 (1994); J. König, J. Schmid, H. Schoeller, and G. Schön, *ibid.* **54**, 16820 (1996).
[22] A. Thielmann, M. H. Hettler, J. König, and G. Schön, Phys. Rev. Lett. **95**, 146806 (2005); Phys. Rev. B **68**, 115105 (2003).
[23] E. V. Sukhorukov, G. Burkard, and D. Loss, Phys. Rev. B **63**, 125315 (2001).
[24] W. Liang, M. Bockrath, and H. Park, Phys. Rev. Lett. **88**, 126801 (2002).
[25] I. Weymann, Europhys. Lett. **76**, 1200 (2006).
[26] Ya. M. Blanter and M. Büttiker, Phys. Rep. **336**, 1 (2000).
[27] S. Gustavsson, R. Leturcq, B. Simovic, R. Schleser, P. Studerus, T. Ihn, K. Ensslin, D. C. Driscoll, and A. C. Gossard, Phys. Rev. B **74**, 195305 (2006).
[28] E. Onac, F. Balestro, B. Trauzettel, C. F. J. Lodewijk, and L. P. Kouwenhoven, Phys. Rev. Lett. **96**, 026803 (2006).
[29] Yiming Zhang, L. DiCarlo, D. T. McClure, M. Yamamoto, S. Tarucha, C. M. Marcus, M. P. Hanson, and A. C. Gossard, Phys. Rev. Lett. **99**, 036603 (2007).